Int. J. Electrochem. Sci., 7 **(2012)** 2890 - 2903

International Journal of
ELECTROCHEMICAL
SCIENCE
www.electrochemsci.org

Bioactivation of 304 Stainless Steel Surface through 45S5 Bioglass Coating for Biomedical Applications

Seyed Morteza Naghib, Mojtaba Ansari[*], *Ali Pedram, Fathollah Moztarzadeh, Masood Mozafari*

Faculty of Biomedical Engineering, Amirkabir University of Technology, P.O. Box 15875-4413, Tehran, Iran.
[*]E-mail: M_ansari@aut.ac.ir

Received: 28 December 2011 / *Accepted:* 17 February 2012 / *Published:* 1 April 2012

The ability of 45S5 bioactive-glass to form a bond to living bone tissue and stimulate bone-cell proliferation may be different for melt- and sol–gel-derived samples. In this research, the differences in corrosion resistance, bioactivity and physical properties between the melt- and sol–gel-derived 45S5 bioglass coated on the surface of austenitic 304 stainless steel (SS) as a dental and orthopedic metallic implant were studied. The morphologies of different coated samples were investigated by scanning electron microscopy (SEM). Then, electrochemical measurements were performed and compared with un-coated ones. In order to investigate the bioactivity and surface reactivity of the coated samples, they were studied in vitro in simulated body fluid (SBF), and their microstructures and electrochemical properties were examined in detail. Immediately after immersion in SBF, reactions occurred on the surface of coated samples, and the obtained results from X-ray powder diffraction (XRD) and Fourier transform infrared spectroscopy (FTIR) analyses showed all typical characteristic peaks of hydroxyapatite (HA). In addition, the coated samples showed an enhanced corrosion resistance and also bioactivity in comparison with un-coated ones, and it is worth mentioning that the sol–gel-derived coated sample showed a higher corrosion resistance and faster forming of the HA layer, which can be useful for dental and orthopedic metallic implants.

Keywords: 304 austenitic stainless steel; 45S5 bioactive-glasse; bioglass coating; melting technique; sol-gel, hydroxyapatite.

1. INTRODUCTION

Metals in different types and shapes are used to make implants, which have many industrial and orthopedic applications due to their desirable mechanical properties, strength, corrosion resistance, mechanical workability [1,2]. The main characteristic of metals and alloys is their favorable mechanical properties. However, there are concerns about their corrosion resistance upon the body

physiologic fluids and also their bioactivity. On the other hand, bioinert metals and alloys are not capable of forming a suitable bond between the implant and tissues [3]. For this reason, developing the techniques for increasing their corrosion resistance and bioactivity seems significant. One of the mentioned techniques is the application of coatings prepared by different methods (such as sol–gel method) [4–14].

Grade 304 SS is one of the useful alloys which are often used as orthopedic implants due to their corrosion resistance, impact resistance, long-term value, strength to weight advantages, hygiene, ease of fabrication and aesthetic appearance. During the these years, many surface modification and coating methods, such as sol–gel, EPD, thermal spraying, arc ion plating, sputtering, etc., have been used to improve the surface characteristics of stainless steels for biomedical applications [15–19]. Some of the most important coatings used in these methods are Ti, TiN, TiO_2, TaC_xN_{1-x}, wollastonite, porcelain, silica and bioactive-glass based layers. In the range of ceramic materials, and according to their nanostructure, bioactive glasses (amorphous solid materials) are placed at the farthest end from the conventional ceramics (crystalline solid materials). Bioactive glasses are a class of bioactive ceramics that are combinations of silicon, sodium, potassium, calcium, phosphorous and magnesium oxides, which show good adhesion to metals because of their high thermal expansion coefficients. They increase the probability of formation of HA (inorganic component of natural bone) on the surface of biomaterials [20–23]. These glasses meet three important features for the coatings of implants and scaffolds: high osteoconductivity and bioactivity, ability to deliver cells and controllable biodegradability [24–33]. Calcium-silico-phosphate glasses have potential as biomaterials for human body because of their bioactivity and biocompatibility. Hench [3] has reported the first bioactive glass having composition (wt.%) 45% SiO_2, 24.5% Na_2O, 24.5% CaO and 6% P_2O_5 commonly known as 45S5 which had been previously coated on 304 SS using electrophoretic deposition [19]. 45S5 bioactive-glass can be prepared via sol–gel and melting techniques, which may have a great influence on the properties of this material.

There are several advantages of a sol–gel-derived glass over a melt-derived glass which are important for dental and orthopedic applications. Sol–gel-derived glasses have the potential of improved purity and homogeneity required for optimal bioactivity due to low processing temperatures (600–700 °C). They also have interconnected nanometer scale porosities that can be varied to control dissolution kinetics or be impregnated with biologically active phases such as growth factors. In addition, they can be foamed to provide interconnected pores of 10–200 μm, mimicking the architecture of trabecular bone. The purpose of the present research is coating of 304 SS with 45S5 bioglass using sol–gel method which is a simpler and cheaper method in comparison with other utilized techniques. For this purpose the prepared sample coated by sol–gel method was compared with a sample coated by melting technique. Finally, the bioactivity of the prepared samples was evaluated by in vitro experiment in SBF solution. In order to coat the 304 SS using the melting method, a suspension of the 45S5 bioglass powder was prepared. The suspension was made from 1 mol of the powder, 10 mol of distilled water and citric acid (0.1 mol%) as dispersant, and then stirred for 1 h. The prepared suspension was sprayed on the surface of the 304 SS specimens. During the coating procedure, steel specimens were kept at 300 °C to evaporate the water of suspension. At the end of the precipitation (coating) process, the coated specimens were heated up to 500 °C for 3 h and 20 min

(with 1 °C/min rate) and kept there for 2 h. They were then heated up to 700 °C for 3 h and 20 min (with 1 °C/min rate) and kept at this point for 40 min. The specimens were cooled slowly in furnace until room temperature. Following the coating of 304 SS using sol–gel technique, the specimens were immersed in the prepared sol for 30 min. After the immersion period, specimens were withdrawn from the sol with a constant velocity of 4 cm/min to let a thin homogenous coating form on the steel surface. The coated specimens were kept at room temperature for 30 min and then heated in furnace up to 500 °C for 8 h (with 1 °C/min rate) and kept there for 2 h. Afterwards, they were heated from 500 °C to 700 °C for 3 h and 20 min (with 1 °C/min rate) and kept at this point for 40 min. The specimens were cooled slowly in furnace until room temperature.

2. EXPERIMENTAL

2.1. Synthesis of 45S5 bioactive-glass via sol–gel technique

The chemical composition of 45S5 bioglass is presented in Table 1 In order to synthesize 45S5 bioglass via sol–gel method, initially, 102.88 cm^3 of tetraethoxysilane (TEOS) was added to 50 cm^3 of 0.1 M nitric acid, and then placed on a stirrer for the hydrolysis process to be performed. At this stage, nitric acid was used as the sol environment and TEOS was utilized as a source to supply SiO_2. Then, 8.861 cm^3 of triethylphosphate (TEP) was added to the system as the P_2O_5 supply, which was then stirred for 45 min. The process was continued by addition of 63.52 g of calcium nitrate tetrahydrate powder, which was previously solved in distilled water as the CaO supply, and again a 45 min period of stirring. The last stage was adding 25.864 g of sodium carbonate (as Na_2O supply, previously solved in distilled water) and placing the whole system on a stirrer for 1 h for complete hydrolysis reactions to occur. The molar ratio of water to TEOS (H_2O:TEOS) was chosen as equal to 12:1. The obtained sol was put in an oven for 6 h at 60 °C, in order to approach to the gel state and become suitable for coating on the surface of steel samples.

2.2. Synthesis of 45S5 bioactive-glass via melting technique

In order to produce 45S5 bioglass via melting technique with the chemical composition mentioned in Table 1, SiO_2, P_2O_5, $CaCO_3$ and Na_2CO_3 powders were blended homogenously. The obtained blend was decarburized at 900 °C for 2 h, and then melted in an alumina plant at 1350 °C for 2.5 h and then quenched in water at room temperature. Afterwards, the produced 45S5 bioglass was milled using planetary milling (SVD15IG5-1, LG Company) for 12 h with 1500 rpm velocity in order to gain the bioactive-glass powder. The fabricated powder was screened to achieve a maximum particle size of 38 μm.

2.3. Substrates and coatings

In this research, 304 SS sheets in 2×2×0.3 cm dimensions were used as substrates. Before applying the coating layers on the surfaces of samples, the specimens were sand blasted and then shot

blasted to improve the roughness of surfaces. Afterwards, they were cleaned by immersing in ethanol to become ready for coating.

Table 1. Chemical composition of 45S5 bioactive-glass in mole and weight percent.

	SiO_2	CaO	Na_2O	P_2O_5
mol %	46.1	26.9	24.4	2.6
wt %	45	24.5	24.5	6

In order to coat the 304 SS using the melting method, a suspension of the 45S5 bioglass powder was prepared. The suspension was made from 1 mol of the powder, 10 mol of distilled water and citric acid (0.1 mol%) as dispersant, and then stirred for 1 h. The prepared suspension was sprayed on the surface of the 304 SS specimens. During the coating procedure, steel specimens were kept at 300 °C to evaporate the water of suspension. At the end of the precipitation (coating) process, the coated specimens were heated up to 500 °C for 3 h and 20 min (with 1 °C/min rate) and kept there for 2 h. They were then heated up to 700 °C for 3 h and 20 min (with 1 °C/min rate) and kept at this point for 40 min. The specimens were cooled slowly in furnace until room temperature. Following the coating of 304 SS using sol–gel technique, the specimens were immersed in the prepared sol for 30 min. After the immersion period, specimens were withdrawn from the sol with a constant velocity of 4 cm/min to let a thin homogenous coating form on the steel surface. The coated specimens were kept at room temperature for 30 min and then heated in furnace up to 500 °C for 8 h (with 1 °C/min rate) and kept there for 2 h. Afterwards, they were heated from 500 °C to 700 °C for 3 h and 20 min (with 1 °C/min rate) and kept at this point for 40 min. The specimens were cooled slowly in furnace until room temperature.

2.3.1. Sintering process

The sintering process which was used at the mentioned temperatures has recently been used in similar researches, usually contributed to sensitization, which had a chemical effect on the structure of stainless steel that might deteriorate some of its properties such as appropriate corrosion resistance and mechanical properties [34,42]. Herein, due to the presence of the coatings, this effect did not significantly reduce the corrosion resistance of the specimens. The related potentiodynamic polarization curves are presented in the next sections. On the other hand, recent researches have indicated that such a heat-treatment would deteriorate the mechanical properties of 304 SS by reducing its fracture toughness (KIC) [35] but this would not still negatively affect the results of this research, since the maximum required mechanical properties for an orthopedic implant is less than the deteriorated properties of a sensitized stainless steel in its worst conditions. For instance, the maximum required tensile strength for a cortical bone is less than 150 MPa which is lower than the ultimate tensile strength of a sensitized stainless steel. Therefore, the utilized heat-treatment in sintering of the coating would not limit the applications of this biomaterial as an orthopedic implant, even if it reduces

the quality of stainless steel. The purpose of such researches is obtaining the best conditions for the coating, ignoring the substrate. However, if the best mechanical conditions were required for the steel substrate, substituting paths of heat-treatment could be used [20].

2.4. Preparation of SBF solution

The SBF solution was prepared by dissolving reagent-grade NaCl, KCl, $NaHCO_3$, $MgCl_2 \cdot 6H_2O$, $CaCl_2$ and KH_2PO_4 into distilled water and buffered at pH=7.25 with TRIS (trishydroxymethyl aminomethane) and HCl 1N at 37 °C. Its composition is given in Table 2 and is compared with the human blood plasma.

2.5. Characterization

2.5.1. XRD and FTIR analysis

XRD analysis (Philips X'Pert-MPD system with a Cu Kα wavelength of 1.5418 Å) was used to analyze the crystal structure and phase present in the coated samples after immersing in SBF. The diffractometry was operated at 40 kV and 30 mA at the 2θ range of 20–55° employing a step size of 0.02°/s. 2.5.2. FTIR analysis FTIR analysis (Bomem, MB-100) was used to observe functional groups developed in the specimens and specially investigated the formation of apatite layer on the surface of 304 SS coated by 45S5 bioactive-glass which was immersed in SBF at 37 °C for 14 days. The FTIR spectra were investigated in the 400–4000 cm^{-1} range.

Table 2. Ion concentrations of simulated body fluid (SBF) and human blood plasma.

Ion	Plasma (mmol/l)	SBF(mmol/l)
Na^+	142.0	142.0
K^+	5.0	5.0
Mg^{2+}	1.5	1.5
Ca^{2+}	2.5	2.5
Cl^-	103.0	103.0
HCO_3	27	27
HPO_4^{2-}	1.0	1.0
SO_4^{2-}	0.5	0.5

2.5.3. SEM observations

SEM analysis (Phillips XL 30) was used to observe the structure and morphology of the 45S5 bioactive-glass coating produced by both techniques on the 304 SS samples.

2.6. In vitro bioactivity testing

Investigating the bioactivity of the metallic implants made of 304 SS coated by 45S5 bioactive-glass layers was performed by imprisoning in SBF solution. The coated specimens were immersed in 100 ml of SBF for 14 days in an incubator at 37 °C. They were then brought out from the incubator and desiccated at room temperature.

2.7. Corrosion behavior evaluation

Potentiodynamic techniques have typically been used for getting qualitative and quantitative information about the electrochemical reactions [36,37]. The electrochemical evaluations were performed to investigate the corrosion behavior of SS 304 uncoated and coated by 45S5 bioglass using melting and sol–gel techniques. To achieve this purpose, specimens were immersed in SBF (as electrolyte) at 37±1 °C (the body temperature). The reference electrode (saturated calomel electrode) was connected to a Pt electrode, and then placed in SBF solution. The specimens and reference electrode were connected to a potentiostat instrument (using an EG&G model 263A potentiostat/galvanostat interfaced with a computer and a recorder) and the corrosion polarization curves were plotted after 2 h for the corrosion reaction to get to equilibrium state. Afterwards, the mean value of corrosion current density and corrosion potential of different specimens were measured from polarization curves using linear polarization and Tafel extrapolation techniques. In addition, standard test deviation of corrosion current density and corrosion potential was calculated (Table 2).

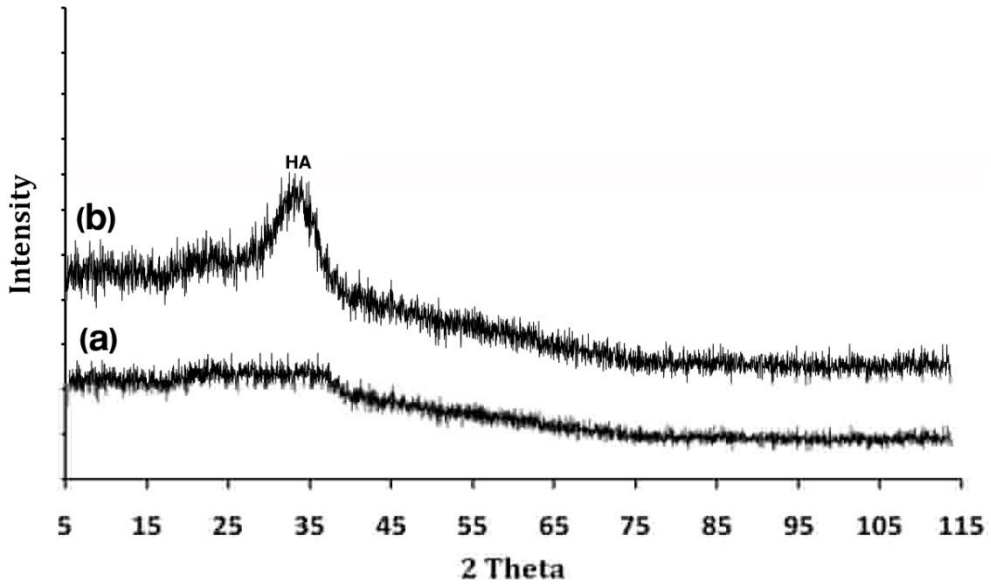

Figure 1. XRD patterns of the surface of melt-derived 45S5 bioactive-glass coated sample (a) before and (b) after 14 days of immersion in SBF.

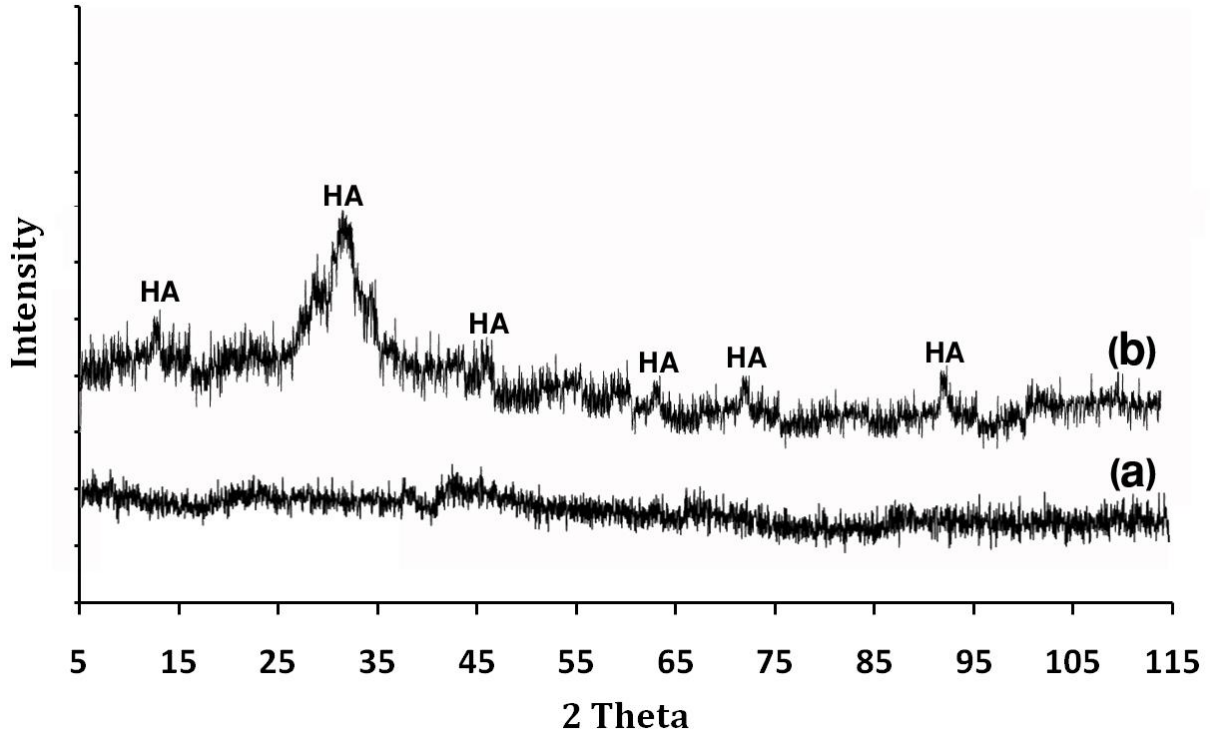

Figure 2. XRD patterns of the surface of sol–gel-derived 45S5 bioactive-glass coated sample (a) before and (b) after 14 days of immersion in SBF.

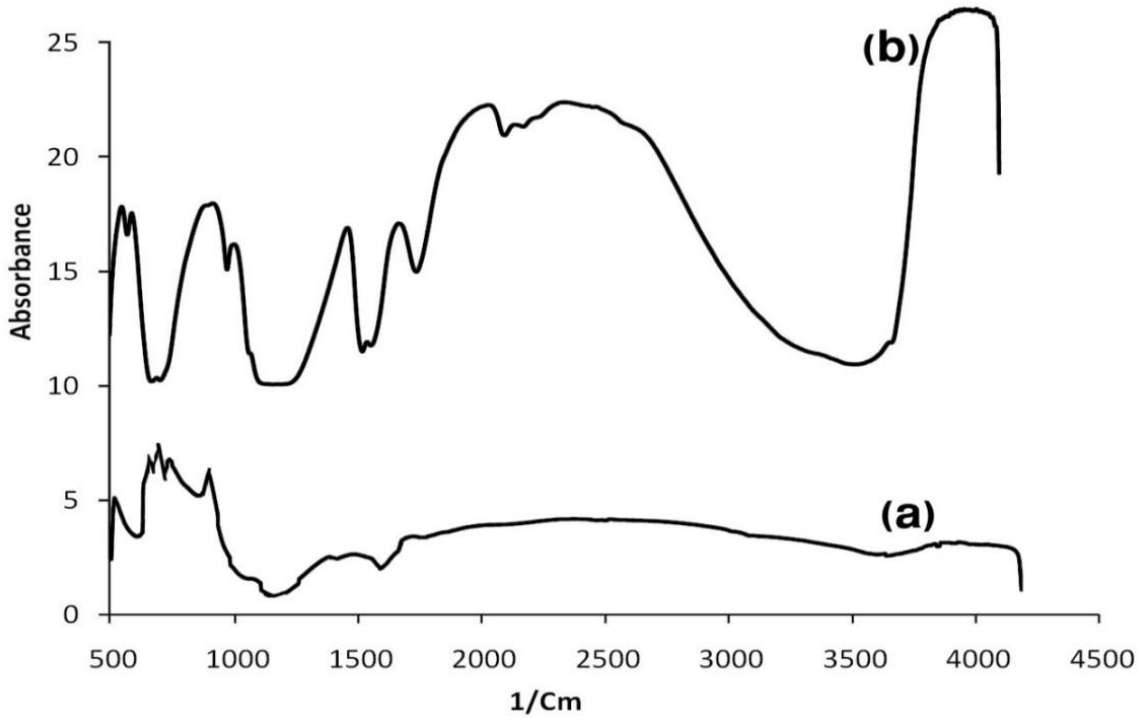

Figure 3. FTIR spectra of the melt-derived 45S5 bioactive-glass coated 304 SS (a) before and (b) after 14 days of immersion in SBF.

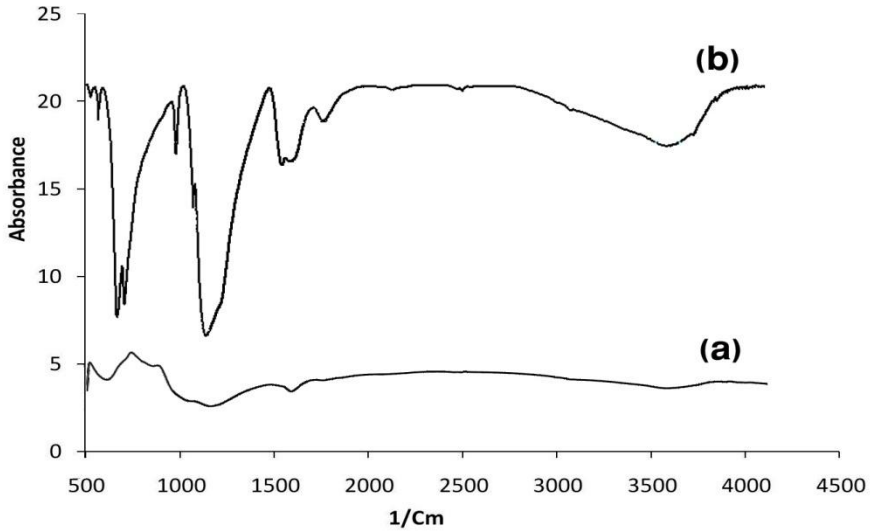

Figure 4. FTIR spectra of the sol–gel-derived 45S5 bioactive-glass coated 304 SS (a) before and (b) after 14 days of immersion in SBF.

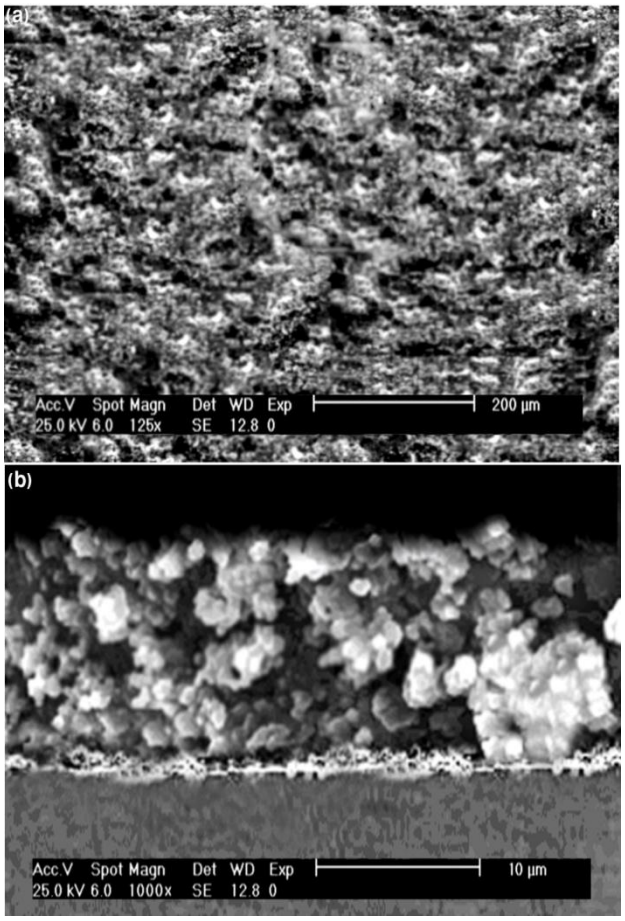

Figure 5. (a) SEM micrograph of the surface of 304 SS coated by melt-derived 45S5 bioactive-glass, (b) SEM micrograph of cross section of 304 SS coated by melt-derived 45S5 bioactive-glass, before immersion in SBF.

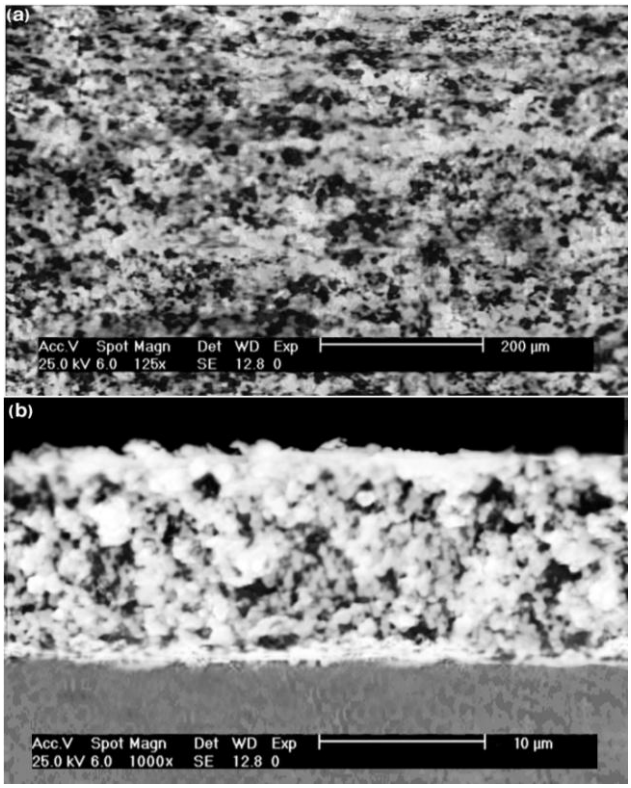

Figure 6. (a) SEM micrograph of the surface of 304 SS coated by sol-gel-derived 45S5 bioactive-glass, (b) SEM micrograph of cross section of 304 SS coated by sol-gel-derived 45S5 bioactive-glass, before immersion in SBF.

3. RESULTS AND DISCUSSION

3.1. Crystal structure and bioactivity

The XRD patterns of melt-derived and sol–gel-derived coated surfaces before and after immersion in SBF solution are shown in Figs. 1 and 2, respectively. In the untreated patterns of both samples, they almost took an amorphous state indicative of the internal disorder and glassy nature of these materials and it is worth mentioning that the applied coating surfaces did not show any crystalline states as shown in Figs. 1(a) and 2(a)As it can be seen in Fig. 1(b) for melt-derived coated sample after immersion in SBF, the XRD results indicated the formation of HA on the surface of samples according to 26° and 32° peaks that are assigned to be (211) and (002) planes of apatite crystals due to the standard JCPDS cards (No. 09-0432). According to Fig. 2, it is important to point out that for the sol–gel-derived coated sample after immersion in SBF, the other peaks of apatite at 39°, 46° and 56° appeared, so additional diffraction peaks may confirm the better formation of the apatite phase in comparison with melt-derived coated sample. The formation of HA layers was also confirmed by FTIR analysis, which is presented in Figs. 3 and 4 for melting and sol–gel techniques, respectively.

After 14 days of immersing the specimens in SBF, the FTIR spectroscopy patterns of both samples showed large peaks at the wave number range of 1000–1200 cm^{-1}, which proved the

formation of an amorphous rich-layer of CaO and P_2O_5. In addition, a peak related to P–O bond was observed at the wave number range of 500–600 cm^{-1}, which showed the formation of HA layer on the surfaces of coated samples [38]. The obtained peaks at the range of 3400–3500 cm^{-1} were associated to the absorbed water in the system. As it can be seen in Fig. 4 for the sol–gel-derived coated sample, the intensities of bands associated to phosphate group vibrations increased and the spectrum became quite similar to that of HA. The characteristic bonds exhibited in the sample's spectra assigned here are the following: Two bonds were observed at 3460 and 673 cm^{-1} due to the stretching mode of hydrogen-bonded OH^- ions and liberational mode of hydrogen-bonded OH^- ions, respectively. The bond at 1131 cm^{-1} arises from υ3 PO_4 and the bond at 604 arises from υ4 PO_4 [39,40]. It is worth mentioning that the larger peaks of P–O bond in FTIR analysis for sol–gel-derived 45S5 bioactive-glass coated sample in comparison with the peaks for melt-derived 45S5 bioglass coated sample can imply the better or faster formation of HA layer on the sol–gel prepared surface.

3.2. SEM observations

At this stage, the morphology and microstructure of the specimens were investigated to see if a perfect and a suitable surface has been formed.

Therefore, the micrographs from surfaces and cross sections of the specimens were taken after coating (before and after 14 days immersion in SBF). As it can be seen in Fig. 5 (a) crack-less and homogeneous coating was not obtained and lots of defects were on the surface. Comparing the SEM micrographs of coated surfaces before immersing in SBF showed that the specimens coated by sol–gel method, as shown in Fig. 6 (a), had more homogenous and uniform surfaces than the specimens coated by 45S5 bioactive-glass produced by melting technique. Furthermore, some pores and cracks could be observed on the specimens coated by the bioglass produced by melting technique, while the specimens coated by sol–gel method show surfaces less of pores and cracks. In addition, as it can be seen in Figs. 5(b) and 6(b) SEM micrographs of the cross sections of specimens before immersion in SBF indicated that the coating thickness of the specimens coated by sol–gel technique is more homogenous and uniform than the same property of the other specimen.

According to Garcia et al. [41], the bioglass coating on the surface of SS samples has a critical thickness, defined as the greatest thickness without cracks, more than 5 μm [5]. It is worth to note that the coating thickness on all the specimens in this research was about 10–15 μm (Figs.5-b and Figs.6-b).

3.3. In vitro assessment in SBF solution

The SEM micrographs of the surface of 304 SS coated by 45S5 bioglass using both melting and sol–gel techniques after 14 days immersion in SBF are presented in Fig. 7(a) and (b), respectively. The difference between the HA layers formed on the coatings produced by two different techniques could be clearly defined. The HA layer formed on the coating produced by sol–gel technique showed

more perfect and homogeneous surface, whereas a porous and a heterogeneous surface in micro-scale is formed on the other specimen.

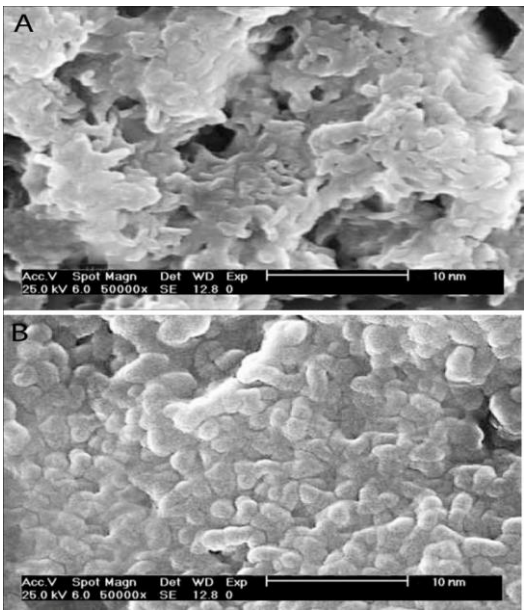

Figure 7. SEM micrographs of the surface of 304 SS coated by (A) melt-derived and (B) sol–gel-derived 45S5 bioglass, after 14 days of immersion in SBF.

3.4. Electrochemical evaluations

The potentiodynamic polarization curves of uncoated and coated 304 SS specimens by bioactive-glass prepared through melting and sol–gel techniques before and after 14 days immersion at 37±1 °C (body temperature) are presented in Fig. 8.

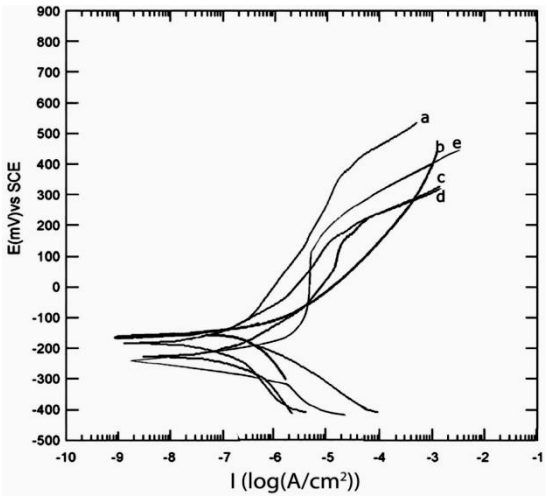

Figure 8. The potentiodynamic polarization curves of 304 SS (a) uncoated, (b) melt-derived coated sample before immersion in SBF, (c) sol–gel-derived coated sample before immersion in SBF, (d) melt-derived coated sample after 14 days of immersing in SBF, and (e) sol–gel-derived coated sample after 14 days of immersion in SBF at 37±1 °C.

Table 3. Mean values (standard deviation) of corrosion current densities and corrosion potentials of the coated and uncoated samples in SBF at 37±1 °C.

Kind of coating	E_{corr}(mV)	I_{corr} (nA/cm^2)	
		Tafel	linear
SS 304 without coating	-156 (20)	242 (16)	188 (20)
SS 304 coated using bioactive-glass produced by melting technique before immersion in SBF	-180 (20)	194 (16)	151 (16)
SS 304 coated by sol-gel method before immersion in SBF	-212 (20)	101 (8)	72 (8)
SS 304 coated using bioactive-glass produced by melting technique after 14 days of immersing in SBF	-194 (20)	128 (12)	98 (10)
SS 304 coated by sol-gel method after 14 days of immersion in SBF	-230 (20)	94 (6)	61 (8)

In addition, Table 3 represents the data extracted from the polarization curves, from which some discussions about the results would be conducted. Also, current densities were calculated using both linear and Tafel extrapolation methods. Comparing the values of corrosion current densities and corrosion potentials of uncoated and coated samples showed that applying the coating layers significantly improved the corrosion resistance of the steel samples in SBF environment at 37±1 °C. This is because of applying the bioglass coating which acts as a barrier against the diffusion of electrolyte and thus postpones the corrosive reactions. Furthermore, an improvement was also observed in the corrosion behavior of 304 SS coated by sol–gel method in comparison with the coated sample by melting method. (i_{corr}=101 nA cm^{-2} and E_{corr}=−212 mV in comparison with i_{corr}=194 nA cm^{-2} and E_{corr}=−180 mV). This is due to the formation of a pore-less coating layer by sol–gel method which is also homogenous and uniform. On the other hand, comparing the values of corrosion current and corrosion potential of the coated samples before and after 14 days immersion in SBF, showed a bit increase in the corrosion resistance of the second group (i_{corr}=94 nA cm^{-2} and E_{corr}=−230 mV in comparison with i_{corr}=101 nA cm^{-2} and E_{corr}=−212 mV). In this case, the HA layer on the surface acts as an excess layer and causes a decrease in the diffusion of electrolyte to the steel surface and thus an increase in the corrosion resistance.

4. CONCLUSION

This research revealed that the melt-derived and sol–gel-derived 45S5 bioactive-glass coating layers could attach to the 304 SS substrate but the key point is that a better crack-less and homogeneous coating layer could be obtained by sol–gel technique. All of the coated samples showed a suitable bioactivity after 14 days of immersion in SBF. In addition, the coating layers acted as a barrier against the diffusion of the electrolyte to the surface of the SS samples and improved their corrosion resistance behavior. However, more improvement in the corrosion resistance was observed

in the following cases: The coated sample using sol–gel method versus the coated sample by the bioglass produced by melting technique. The coated samples after 14 days immersion in SBF versus those ones that were not immersed, which was because of the formation of HA layer in addition to 45S5 bioactive-glass on the surface of 304 SS sample.

ACKNOWLEDGEMENT
This research was supported by the School of Biomedical Engineering at Amirkabir University of Technology, and they are gratefully acknowledged.

References

1. C.D. Arrieta-González, J. Porcayo-Calderon, V.M. Salinas-Bravo, J.G. Chacon-Nava, A. Martinez-Villafañe, J.G. Gonzalez-Rodriguez, *Int. J. Electrochem. Sci*, 6 (2011) 3644 – 3655
2. Y. Ait Albrimi, A. Eddib, J. Douch, Y. Berghoute, M. Hamdani, R.M. Souto, *Int. J. Electrochem. Sci*, 6 (2011) 4614 – 4627
3. K. Meinert, C. Uerpmann, J. Matschullat, G.K. Wolf, *Surf. Coat. Technol*, 58 (1998) 103–104
4. O. de Sanctis, L. G´omez, N. Pellegri, C. Parodi, A. Marajofsky, and A. Duran, *J. Non-Cryst. Solids*, 121 (1990) 338–343.
5. M. Mozafari, F. Moztarzadeh, M. Rabiee, M. Azami, M. Tahriri, Z. Moztarzadeh, N. Nezafati, *Ceram. Int*, 2431–2439 (2010) 36.
6. M. Mening, C. Schelle, *A.* Durán, J.J. Damborenea, M. Gugli-. 375 elmi, G. Brusatin, J. *Sol–Gel Sci. Technol. 717* (*1998) 13.*
7. P. Galliano, J.J. de Damborenea, M.J. Pascual, A. Dura n, *J, Sol–Gel Sci. Technol*, 723 (1998) 13.
8. J. Gallardo, P. Galliano, R. Moreno, A. Durán, *J. Sol–Gel Sci. Technol*, 107 (2000) 19.
9. J. Gallardo, P. Galliano, A. Dura n, *J. Sol Gel Sci. Technnol*, 65 (2001) 21.
10. L.L. Hench, '*CRC Handbook of Bioactive Ceramics'*, vol. 1, CRC Press, Boca Raton, Florida, 1982.
11. P.C. Innocenzi, M. Guglielmi, M. Gobbin, P. Colombo, *J. Eur. Ceram. Soc*, 431 (1992) 10.
12. M. Mozafari, F. Moztarzadeh, M. Rabiee, M. Azami, M. Tahriri, Z. Moztarzadeh, *Adv. Comp. Lett*, 91 (2010) 19.
13. M. Mozafari, F. Moztarzadeh, M. Tahriri, *J. Non-Cryst. Solids*, 1470 (2010) 356.
14. L.L. Hench, J.M. Polak, *Science*, 1014 (2002) 295.
15. S.M.Hosseinalipour, A. Ershad-langroudi, H. A. Nemati, A.M.Nabizade-Haghighi, *Prog. Org. Coat*, 371 (2010) 67.
16. H.H. Rodríguez, G. Vargas, D.A. Cortés, *Ceram. Int*, 1303 (2008) 34.
17. C. Liu, LinG. , D. Yang, M. Qi, *Surf. Coat. Technol*, 4011 (2006) 200.
18. M.H. Ding, B.L.Wang, *L. Li and* Y.F. Zheng, *Surf. Coat. Technol*, 2519 (2010) 204.
19. A. R. Boccaccini , C. Peters , J. A. Roether , D. Eifler , S. K. Misra , E. J. Minay, *Surf. Coat. Technol*, 4835 (2006) 200.
20. J. Gallardo, P. Galliano, A. Duran, *J. Sol–Gel Sci. Technol*, 65 (2001) 21.
21. E.M. Santos, S. Radin, P. Ducheyne, *Biomaterials*, 1695 (1999) 20.
22. S. Radin, P. Ducheyne, T. Kamplain, B.H. Tan, *J. Biomed. Mater. Res*, 313 (2001) 57.
23. J. Livage, T. Coradin, C. Roux, *J. Phys. Condens. Matter*, R673 (2001) 13.
24. J. Wilson, G.H. Pigot, F.J. Schoen, L.L. Hench, *J. Biomed. Mater. Res*, 805 (1981) 15.
25. H. O.onishi, S. Kutrshitani, E. Yasukawa, H. Iwaki, L.L. Hench, J. Wilson, E. Tsuji, T. Sugihara, *Clin. Orthop. Relat. Res*, 334 (1997) 316.
26. L.L. Hench, R.J. Splinter, W.C. Allen, *J. Biomed. Mater. Res. Symp*, 117 (1971) 2.

27. L.L. Hench, H.A. Paschall, *J. Biomed. Mater. Res. Symp*, 25 (1973) 4.
28. L.L. Hench, H.A. Paschall, *J. Biomed. Mater. Res. Symp*, 49 (1974) 5.
29. A.M. Gatti, G. Valdre, O.H. Andersson, *Biomaterials*, 208 (1994) 15.
30. A.E. Clark, L.L. Hench, *J. Biomed. Mater. Res*, 693 (1994) 28.
31. L.L. Hench, *Curr. Opin. Solid State Mater. Sci*, 604 (1997) 2.
32. L.L. Hench, J. Wilson, *Science*, 630 (1984) 226.
33. L.L. Hench, J. Wilson, *Science*, 630 (1984) 226.
34. N. Parvathavarthini, R. K. Dayal, *J. Nucl. Mater*, 305 (2002) 209.
35. O.A. Hilders, G. Santana, *Metallography*, 21 (1988) 151.
36. S. M. Naghib, M. Rabiee, E. Omidinia, P. Khoshkenar, *Electroanalysis*, 407 (2012) 24.
37. S. M. Naghib, M. Rabiee, E. Omidinia, P. Khoshkenar, D. Zeini, *Int. J. Electrochem. Sci*, 7 (2012) 407.
38. L.L. Hench, J. Wilson, '*An Introduction to Bioceramic',* World Scientific, Singapore, (1993) p75.
39. M. Mozafari, M. Rabiee, F. Moztarzadeh, M. Azami, S. Maleknia, *Appl. Surf. Sci*, 257 (2010) 1740–1749 .
40. A. Hamlekhan, M. Mozafari, N. Nezafati, M. Azami, H. Hadipour, *Adv. Comp. Lett*, 123 (2010) 19.
41. C. Garcia, S. Cere, A. Duran, *Non-Cryst. Solids*, 348 (2004) 218–224.
42. J.H. Kim, S.K. Kim, Y.Z. You, D.I. Kim, S.T. Hong, *Int. J. Electrochem. Sci*, 6 (2011) 4365 – 4377